Supplemental Data for: Molecular Impact of Covalent Modifications on Nonribosomal Peptide Synthetase Carrier Proteins Communication.

Andrew C. Goodrich[1], David J. Meyers[2], and Dominique P. Frueh[1]

From the Department of Biophysics and Biophysical Chemistry[1] and Department of Pharmacology and Molecular Sciences Synthetic Core[2], Johns Hopkins University School of Medicine, Baltimore, Maryland 21205

STRUCTURE STATISTICS

NMR structure statistics for apo-ArCP	
Violations (mean and s.d.)[a]	
Distance constraints (Å)	0.38 +/- 0.03
Dihedral angle constraints (º)	2.52 +/- 0.56
Max. dihedral angle violation (º)	3.86
Max. distance constraint violation (Å)	0.46
R. m. s. deviations geometry [b]	
Bond lengths (Å)	0.016
Bond angles (º)	1.5
Average pairwise r.m.s.d. [residues 21–90] (Å) [a]	
Heavy	0.94 +/- 0.10
Backbone	0.38 +/- 0.10
Ramachandran Statistics [c]	
Most favoured	93.0
Additionally allowed	7.0
Generously allowed	0.0
Disallowed	0.0

Table S1: NMR structure statistics for apo-ArCP. a) from CYANA 2.1(1), b) From PSVS (2), c) from ProCheck (3).

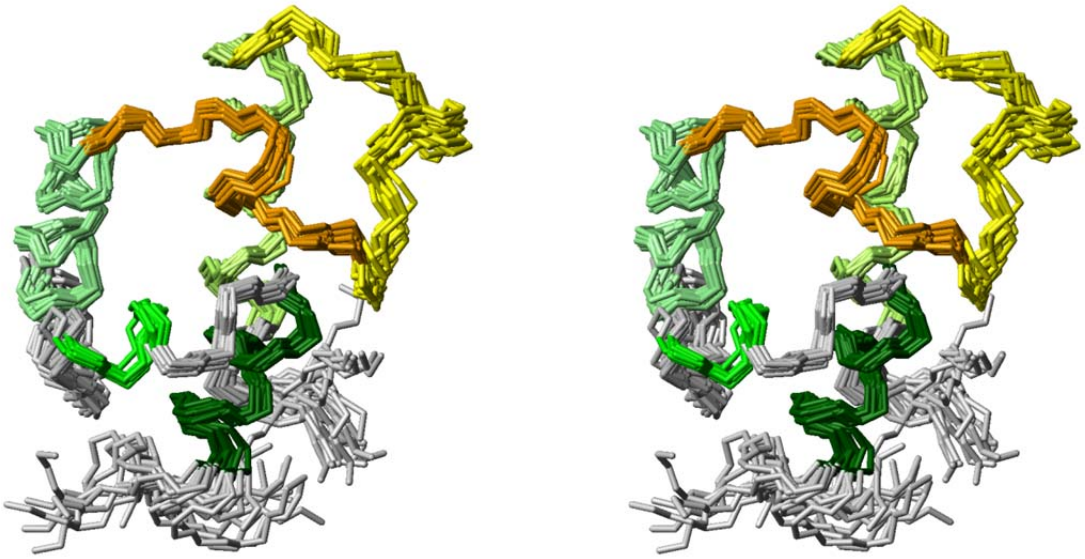

Figure SI 1. Stereoscopic view of the structural bundle of apo-ArCP. Alignments made with C^{α} of residues in helices only (r.m.s.d of 0.39Å). Helices (α1, α2, α3, and α4) are colored from pale green to dark green, respectively. Loop1 is colored in yellow (N-terminal region) and orange (C-terminal region). Figure generated with molmol (4).

Relaxation analysis.

Residue	R_1	σR_1	R_2	σR_2	NOE	σNOE	S^2	σS^2	τ_{loc}	S^2_{fast}	R_{ex}
D14	1.49	0.0275	2.67	0.0845	-0.14535	0.0242	0.177	0.017	9.08E-01	0.781	0
N15	1.65	0.0224	3.07	0.0574	0.13025	0.00808	0.211	0.015	1.16E+00	0.792	0
R16	1.94	0.0303	6.45	0.0677	0.51431	0.00978	0.796	0.009	1.29E-01	1	0
H17	1.97	0.0289	6.61	0.0864	0.68121	0.0116	0.797	0.009	8.94E-01	0.89	0
A18	2.18	0.039	10.53	0.151	0.77061	0.0111	0.96	0.019	4.88E-02	1	2.771
A19	2.1	0.0317	8.85	0.113	0.73104	0.0143	0.917	0.015	6.66E-02	1	1.411
D20	2.06	0.0303	16.53	0.482	0.70931	0.0138	0.895	0.014	7.02E-02	1	9.264
Y21	2.08	0.0286	7.51	0.0817	0.79262	0.0125	0.926	0.008	0.00E+00	1	0
Q22	2.05	0.0259	7.29	0.0816	0.79784	0.0127	0.905	0.008	0.00E+00	1	0
Q23	2	0.0277	7	0.0873	0.77091	0.0136	0.872	0.013	1.45E-02	1	0
L24	2.09	0.0302	7.04	0.0725	0.75826	0.00981	0.857	0.012	1.50E+00	0.914	0
R25	2.06	0.0249	7.43	0.0884	0.7747	0.0126	0.917	0.008	0.00E+00	1	0
E26	1.99	0.028	7.09	0.0946	0.84402	0.0129	0.879	0.009	0.00E+00	1	0
R27	2.03	0.0151	6.51	0.153	0.77217	0.00969	0.847	0.012	1.50E+00	0.893	0
L28	2.05	0.0204	7.23	0.0516	0.72876	0.00872	0.895	0.006	5.13E-02	1	0
I29	1.97	0.0475	9.73	0.621	0.80863	0.0408	0.869	0.022	0.00E+00	1	2.75
Q30	1.96	0.0244	7.41	0.0799	0.75308	0.014	0.86	0.021	2.25E-02	1	0.443
E31	1.95	0.0227	7.63	0.0761	0.80575	0.0111	0.859	0.011	0.00E+00	1	0.735
L32	2.01	0.0303	7.8	0.0846	0.80061	0.0142	0.882	0.015	0.00E+00	1	0.76
N33	2.01	0.0237	6.96	0.0559	0.77894	0.0185	0.849	0.007	1.50E+00	0.887	0
L34	1.83	0.0214	6.69	0.0654	0.75009	0.0186	0.807	0.007	0.00E+00	1	0.2
T35	1.73	0.0154	6.69	0.0531	0.68018	0.00954	0.744	0.02	3.13E-02	1	0.658
Q37	1.96	0.0398	10.29	0.175	0.6847	0.0123	0.846	0.019	5.82E-02	1	3.416
Q38	2	0.0176	7.49	0.049	0.6757	0.00888	0.862	0.018	7.42E-02	1	0.455
L39	1.77	0.0211	6.69	0.0726	0.73255	0.00765	0.801	0.007	2.12E-02	1	0
H40	1.92	0.0262	21.08	0.333	0.69788	0.00942	0.83	0.013	4.46E-02	1	14.348
E42	2.11	0.0456	17.29	0.477	0.84388	0.0209	0.923	0.02	0.00E+00	1	9.948
S43	2.02	0.0459	9.41	0.164	0.79351	0.0162	0.895	0.022	0.00E+00	1	2.178
N44	2.01	0.0254	7.66	0.0877	0.77382	0.011	0.887	0.019	1.32E-02	1	0.488
L45	2.1	0.0285	13.03	0.186	0.78909	0.0144	0.931	0.015	0.00E+00	1	5.502
I46	2.13	0.0216	7.68	0.0558	0.75838	0.0125	0.945	0.013	5.13E-02	1	0
Q47	2	0.035	6.74	0.0803	0.78224	0.018	0.855	0.009	0.00E+00	1	0
A48	1.96	0.0333	7.53	0.14	0.78055	0.0114	0.868	0.015	0.00E+00	1	0.519
G59	1.99	0.0178	7.16	0.062	0.7431	0.0111	0.877	0.006	3.23E-02	1	0
L50	2.08	0.0252	6.82	0.105	0.84334	0.0323	0.84	0.008	1.50E+00	0.908	0

D51	1.67	0.0173	6.03	0.0553	0.67553	0.00991	0.732	0.005	2.97E-02	1	0
S52	1.91	0.0334	7.41	0.123	0.75422	0.0106	0.833	0.03	1.73E-02	1	0.726
I53	1.96	0.0216	7.28	0.0701	0.68938	0.0117	0.845	0.018	5.52E-02	1	0.424
R54	2.01	0.0346	6.9	0.109	0.7465	0.0172	0.834	0.016	1.40E+00	0.893	0
L55	2.16	0.0342	7.42	0.0936	0.75336	0.0144	0.933	0.01	5.11E-02	1	0
M56	1.99	0.032	6.77	0.114	0.76272	0.0138	0.832	0.016	1.49E+00	0.875	0
R57	2.08	0.0294	7.19	0.0878	0.79534	0.0168	0.902	0.009	0.00E+00	1	0
W58	2.1	0.0388	6.83	0.0907	0.77615	0.0165	0.839	0.019	1.50E+00	0.899	0
L59	2	0.0359	7.22	0.0903	0.76855	0.0143	0.891	0.009	1.62E-02	1	0
H60	2.08	0.0352	7.07	0.0772	0.81976	0.0156	0.887	0.009	0.00E+00	1	0
W61	2.1	0.0292	7.46	0.089	0.78254	0.0167	0.926	0.009	0.00E+00	1	0
F62	2.07	0.0342	7.25	0.085	0.78225	0.0167	0.908	0.01	0.00E+00	1	0
R63	2.07	0.03	7.44	0.0798	0.78813	0.0139	0.921	0.008	0.00E+00	1	0
K64	2.06	0.0332	7.48	0.0811	0.78715	0.012	0.921	0.008	0.00E+00	1	0
N65	1.97	0.0183	6.76	0.0601	0.77003	0.012	0.829	0.007	1.49E+00	0.867	0
G66	2.03	0.0198	7.11	0.0569	0.80823	0.00986	0.892	0.008	0.00E+00	1	0
Y67	2.07	0.0197	7.05	0.0621	0.78493	0.0101	0.871	0.006	1.50E+00	0.904	0
R68	1.97	0.0215	6.43	0.0567	0.70122	0.00792	0.785	0.017	1.10E+00	0.873	0
L69	1.83	0.0119	5.33	0.054	0.60208	0.00775	0.604	0.01	1.32E+00	0.816	0
T70	1.99	0.0161	6.69	0.0557	0.79339	0.00915	0.837	0.005	1.49E+00	0.864	0
L71	2.08	0.0404	7.02	0.111	0.79099	0.018	0.893	0.01	0.00E+00	1	0
R72	2.1	0.0303	6.79	0.0834	0.77508	0.0132	0.84	0.013	1.50E+00	0.9	0
E31	2.3	0.111	7.14	0.123	0.83321	0.0555	0.895	0.018	0.00E+00	1	0
L74	1.93	0.0235	6.84	0.0659	0.76102	0.00931	0.848	0.03	1.57E-02	1	0
Y75	1.99	0.0282	7.04	0.0695	0.77211	0.0123	0.876	0.007	1.22E-02	1	0
A76	2.03	0.0298	7.15	0.0834	0.76929	0.0145	0.888	0.009	1.75E-02	1	0
A77	1.85	0.025	7.55	0.0857	0.71719	0.00856	0.805	0.012	2.94E-02	1	1.019
T79	1.94	0.0192	7.62	0.0527	0.7228	0.00979	0.841	0.009	3.49E-02	1	0.835
L80	2.07	0.0264	7.31	0.0911	0.78404	0.0124	0.912	0.009	0.00E+00	1	0
A81	2.06	0.0273	7.65	0.0872	0.7982	0.0135	0.909	0.013	0.00E+00	1	0.351
A82	2.07	0.0404	7.31	0.097	0.77559	0.0176	0.908	0.01	0.00E+00	1	0
W83	2.01	0.0211	7.79	0.0803	0.81597	0.0122	0.888	0.012	0.00E+00	1	0.645
N84	2.02	0.0255	7.24	0.0769	0.8125	0.0133	0.896	0.007	0.00E+00	1	0
Q85	1.93	0.0266	7.25	0.0805	0.78699	0.0114	0.856	0.012	0.00E+00	1	0.33
L86	2.05	0.0381	7.46	0.0992	0.82866	0.0179	0.918	0.01	0.00E+00	1	0
M87	2	0.0258	6.98	0.0756	0.77566	0.0121	0.875	0.007	0.00E+00	1	0
L88	1.99	0.0334	6.34	0.184	0.79447	0.0113	0.853	0.013	0.00E+00	1	0
S89	1.91	0.0201	6.39	0.0533	0.69769	0.00842	0.762	0.016	1.15E+00	0.857	0

R90	2.04	0.0214	6.02	0.0503	0.7056	0.00998	0.718	0.009	1.33E+00	0.868	0
S91	1.96	0.0212	5.18	0.047	0.59978	0.0118	0.571	0.009	1.33E+00	0.847	0
E93	1.55	0.0132	2.92	0.0436	0.06801	0.00458	0.201	0.01	1.08E+00	0.764	0

Table S2. Relaxation parameters and model-free parameters for apo-ArCP. The experimental error for a given parameter is indicated with σ. ROTDIF (5, 6) does not provide experimental errors for τ_{loc}, S_{fast}^2, nor R_{ex}. Dashes indicate when a given model-free parameter was not included in the fit.

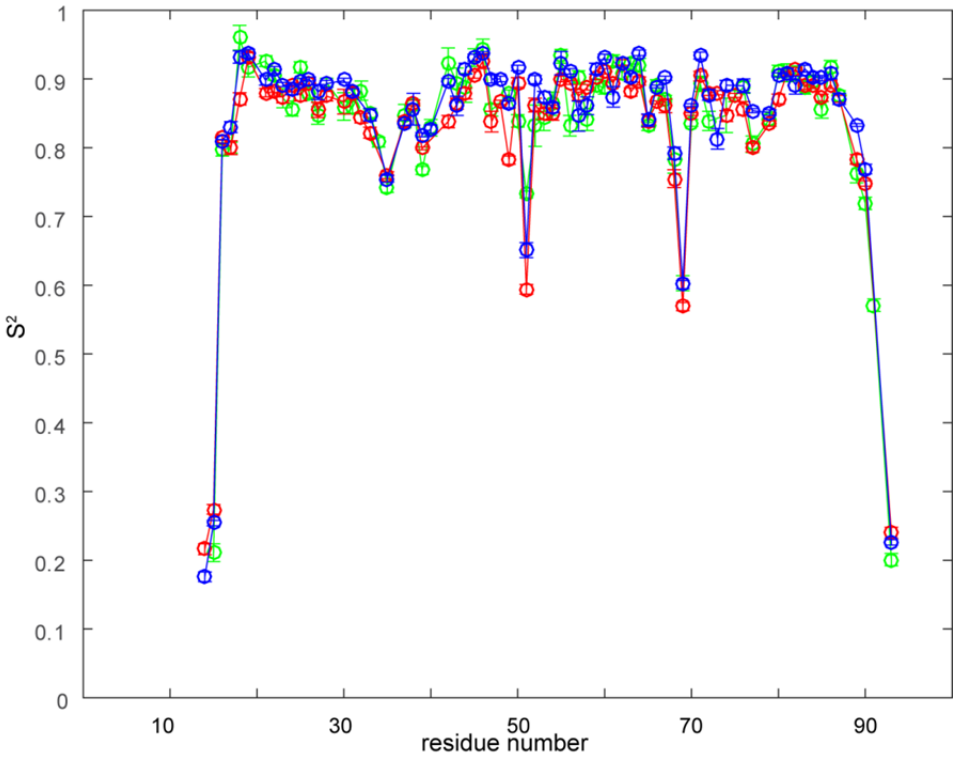

Figure S2: Comparison of order parameters in apo-, holo- and loaded-ArCP. Green: apo, red: holo, blue: loaded.

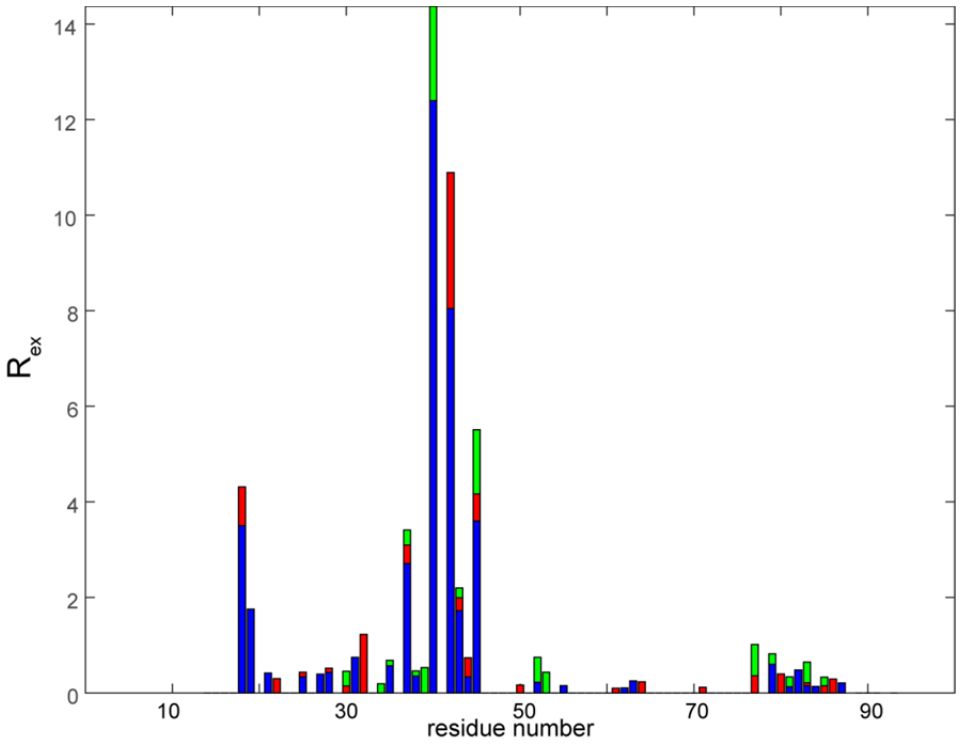

Figure S3: Comparison of exchange rates in apo-, holo- and loaded-ArCP. Green: apo, red: holo, blue: loaded.

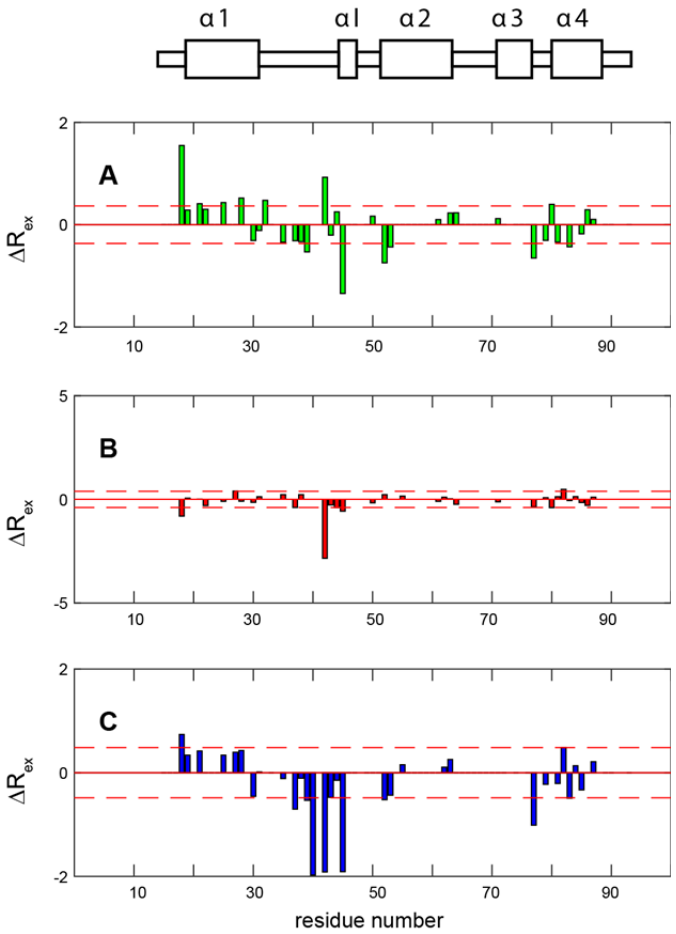

Figure S4. Variations in exchange rates, ΔR_{ex}, between A) holo- and apo-ArCP, B) loaded- and holo-ArCP, and C) loaded- and apo-ArCP. The values of ΔR_{ex} shown here are depicted as color gradients, from white to full-color, in Figure 6 of the main text. The horizontal dashed lines depict the standard deviation of ΔR_{ex}. Residues with values above one standard deviation will appear as hot spots in Figure 6.

Table S3. Confirmation of mutation, post-translational modifications, and fluorescent labeling of ArCP by MALDI-MS

Sample	Calculated Mass (Da)	Experimental Mass (Da)
Apo-ArCP	9758.0	9759.14
Holo-ArCP[a]	10098.35	10094.79
Holo-ArCP•2Na[a]	10144.33	10145.04
SalNH-ArCP[a]	10201.42	10203.61
SalNH-ArCP•4Na[a]	10293.38	10296.56
Apo-ArCP_R16C	9705.03	9706.61
Holo-ArCP_R16C[a]	10045.38	10043.53
FL-Holo-ArCP_R16C[a,b]	10541.78	10541.01
SalNH-ArCP_R16C[a]	10148.45	10150.75
FL-SalNH-ArCP_R16C[a,b]	10644.85	10650.86
$^{15}N^{2}H$-Apo-ArCP[c]	--	10313.81
$^{15}N^{2}H$-Holo-ArCP[a,d]	10674	10681.34
$^{15}N^{2}H$-SalNH-ArCP[a,e]	10756	10763.63

a) Residual apo-ArCP is consistently detected by MALDI but is undetectable in NMR spectra of holo- or SalNH-ArCP under the conditions described in the Experimental Approach, suggesting the level of apo-ArCP is negligible. Well-resolved, intense NMR signals (A77 and S52) were used to probe for apo-ArCP signals by inspecting 1D slices in 2D spectra. The absence of apo-ArCP signals when the signal-to-noise ratios of SalNH-ArCP and holo-ArCP signals reaches 88.2 and 125.4, respectively, indicates that the concentration of apo-ArCP is less than 1% of that of SalNH-ArCP and holo-ArCP. b) Samples tagged with fluorescein maleimide. c) Samples are obtained by expressing the protein in D_2O but protonated glucose is supplied, resulting in fractional deuteration. d) Calculated using experimental

mass of $^{15}N^{2}H$-apo-ArCP plus $^{15}N^{2}H$-labeled phosphopantetheine arm. e) Calculated using experimental mass of $^{15}N^{2}H$-apo-ArCP plus unlabeled ($^{14}N^{1}H$) SalNH-PP.

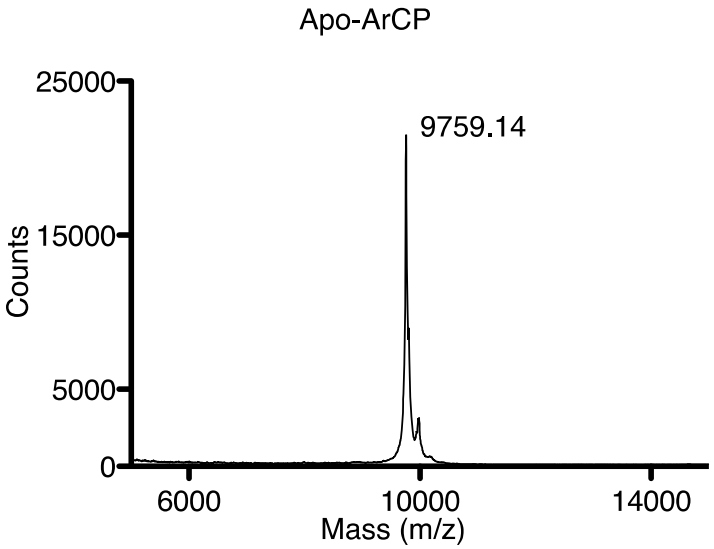

Figure S5. MALDI-MS spectrum of apo-ArCP. Calculated mass: 9758.0. Experimental mass: 9759.14.

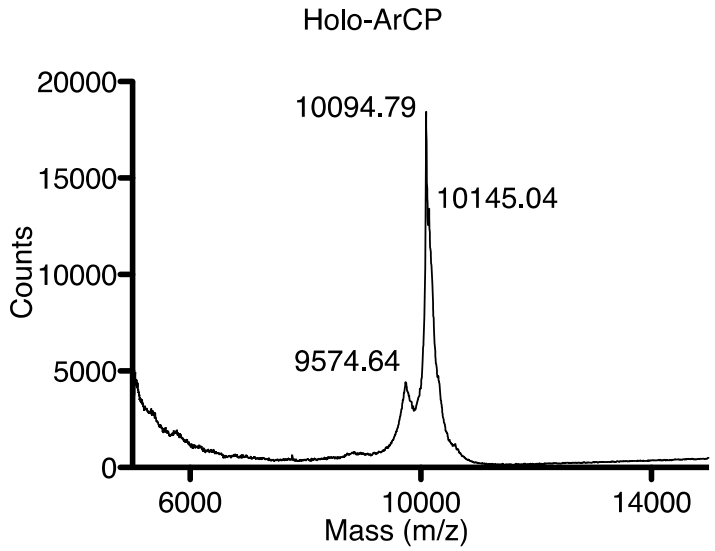

Figure S6. MALDI-MS spectrum of holo-ArCP. Calculated mass holo-ArCP: 10098.35. Experimental mass holo-ArCP: 10094.79. Calculated mass holo-ArCP•2Na: 10144.33. Experimental mass holo-ArCP•2Na: 10145.04.

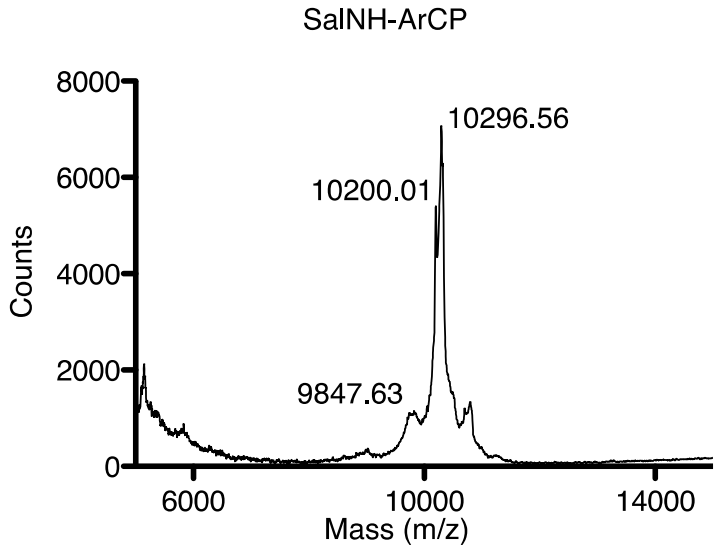

Figure S7. MALDI-MS spectrum of SalNH-ArCP. Calculated mass SalNH-ArCP: 10201.42. Experimental mass SalNH-ArCP: 10200.01. Calculated mass SalNH-ArCP•4Na: 10293.38. Experimental mass SalNH-ArCP•2Na: 10296.56.

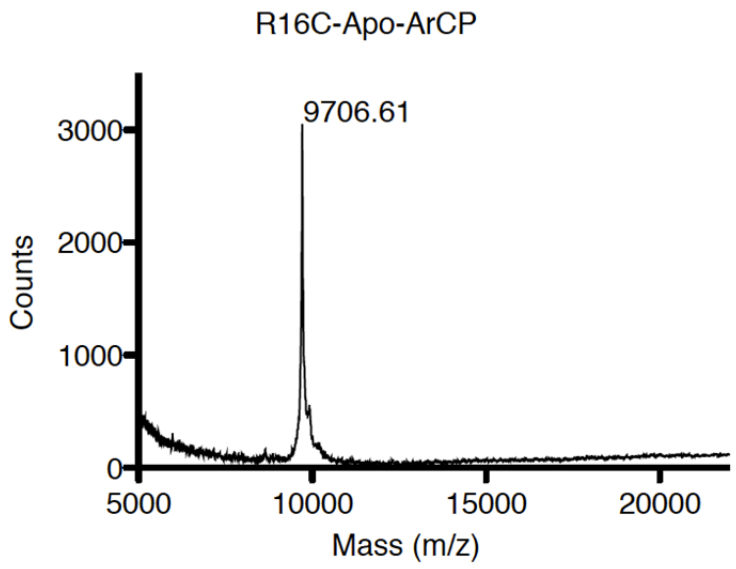

Figure S8. MALDI-MS spectrum of R16C-apo-ArCP. Calculated mass: 9705.03. Experimental mass: 9706.61.

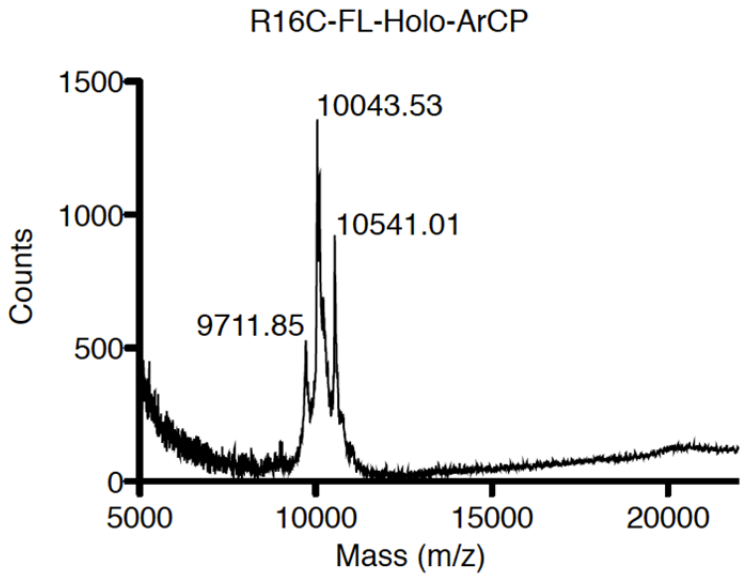

Figure S9. MALDI-MS spectrum of fluorescently labeled R16C-holo-ArCP. Calculated mass, unlabeled: 10045.38. Experimental mass, unlabeled: 10043.53. Calculated mass, labeled: 10541.78. Experimental mass, labeled: 10541.01.

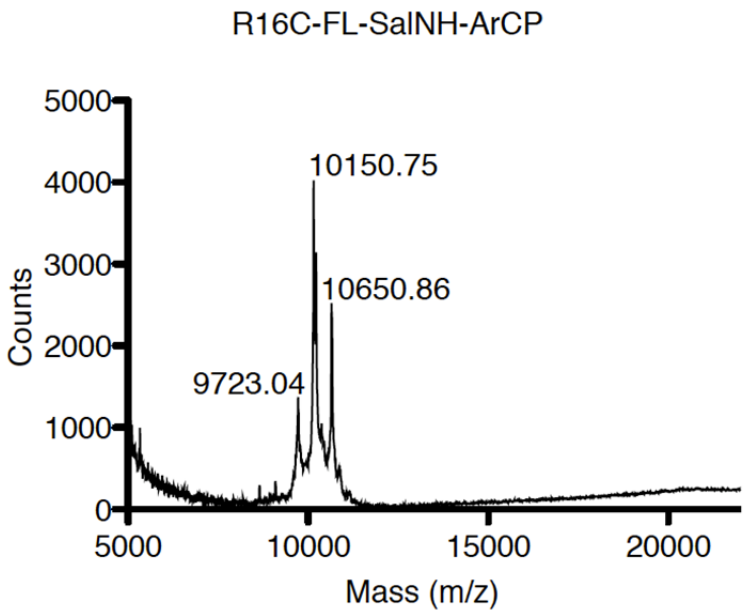

Figure S10. MALDI-MS spectrum of fluorescently labeled R16C-SalNH-ArCP. Calculated mass, unlabeled: 10148.45. Experimental mass, unlabeled: 10150.75. Calculated mass, labeled: 10644.85. Experimental mass, labeled: 10650.86.

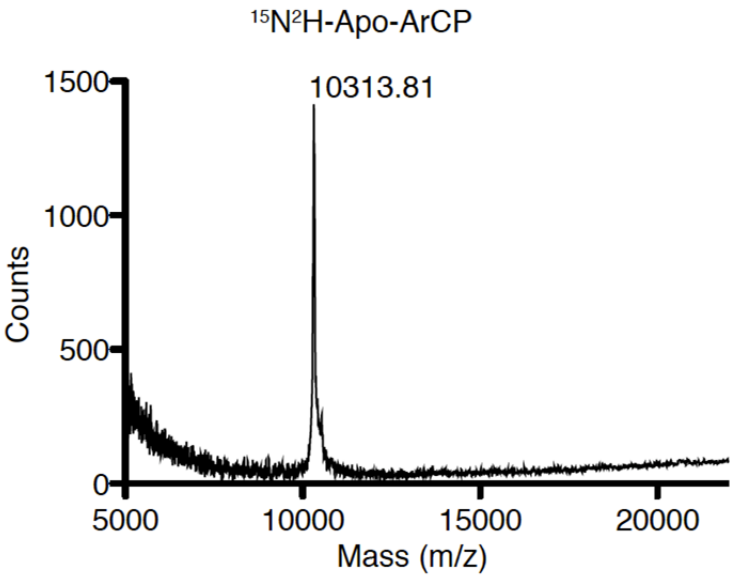

Figure S11. MALDI-MS spectrum of $^{15}N^{2}H$-apo-ArCP. Calculated mass: 10386. Experimental mass: 10313.81. Calculated mass assumes 100% labeling with ^{2}H and ^{15}N.

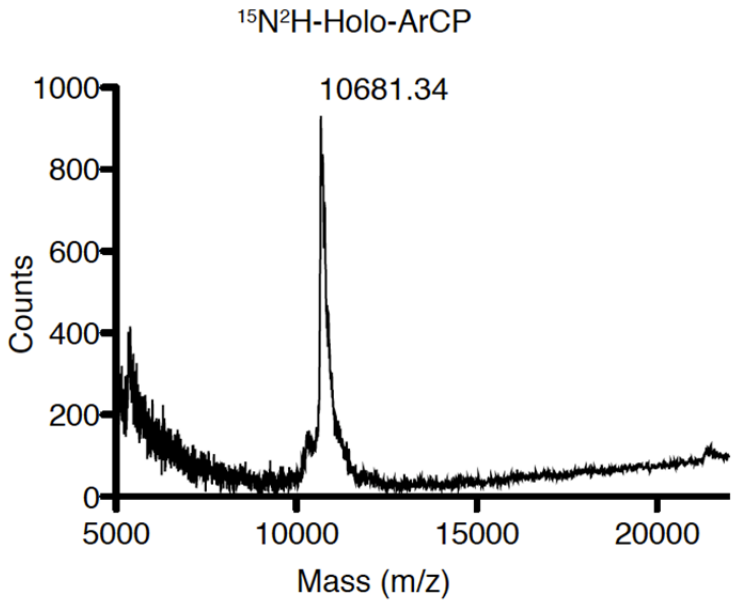

Figure S12. MALDI-MS spectrum of $^{15}N^{2}H$-holo-ArCP. Calculated mass: 10674. Experimental mass: 10681.34. Calculated mass used the measured mass of $^{15}N^{2}H$-apo-ArCP (Figure S11) and $^{15}N^{2}H$-phosphopantetheine.

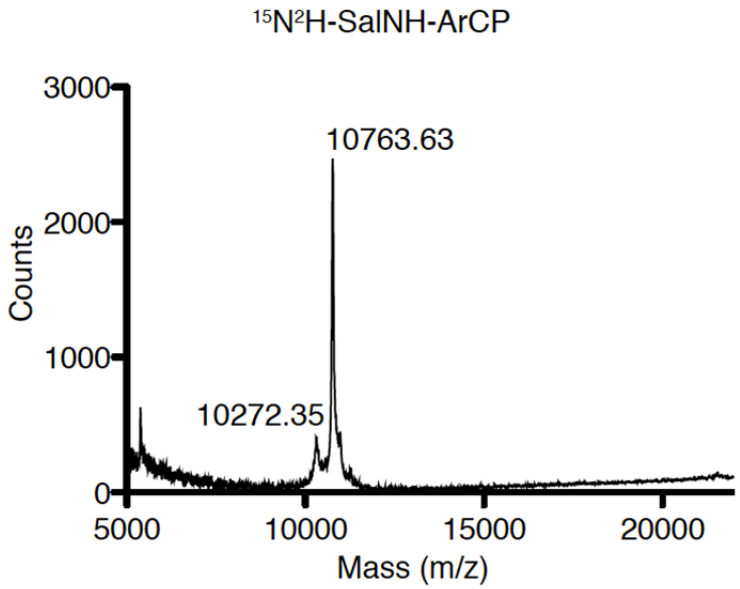

Figure S13. MALDI-MS spectrum of $^{15}N^{2}H$-SalNH-ArCP. Calculated mass: 10756. Experimental mass: 10763.63. Calculated mass used the measured mass of $^{15}N^{2}H$-apo-ArCP (Figure S11) and unlabeled SalNH-PP.

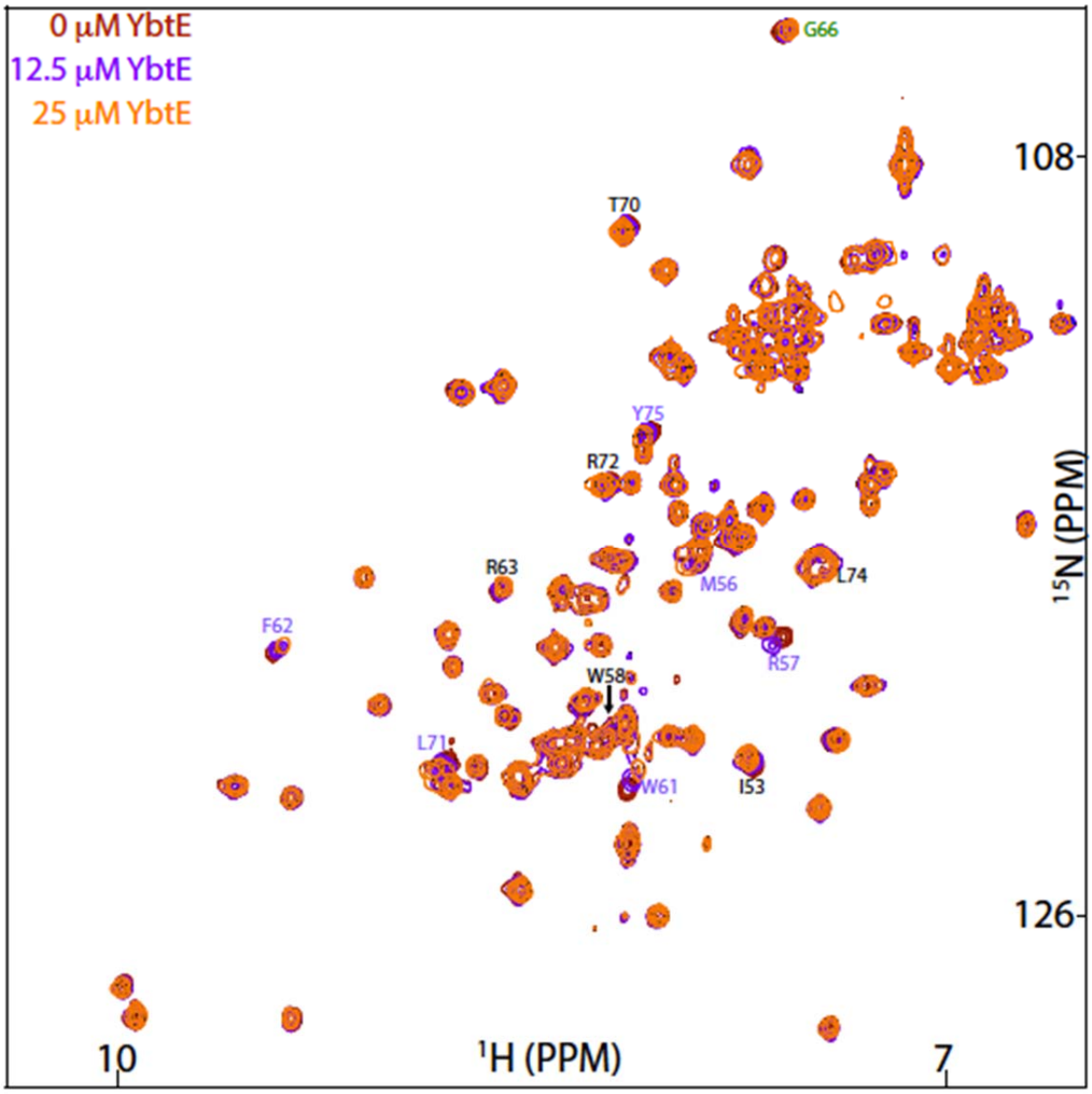

Figure S14. Overlay of HN-HSQCs collected during titration of apo-ArCP with YbtE. Residues that showed a CSP greater than 1 standard deviation (STDEV) above the mean are labeled in black, those that showed a R_{int} greater than 1 STDEV above the mean are labeled in green, and those that showed a CSP and R_{int} that were both greater than 1 STDEV above the mean are labeled in lavender.

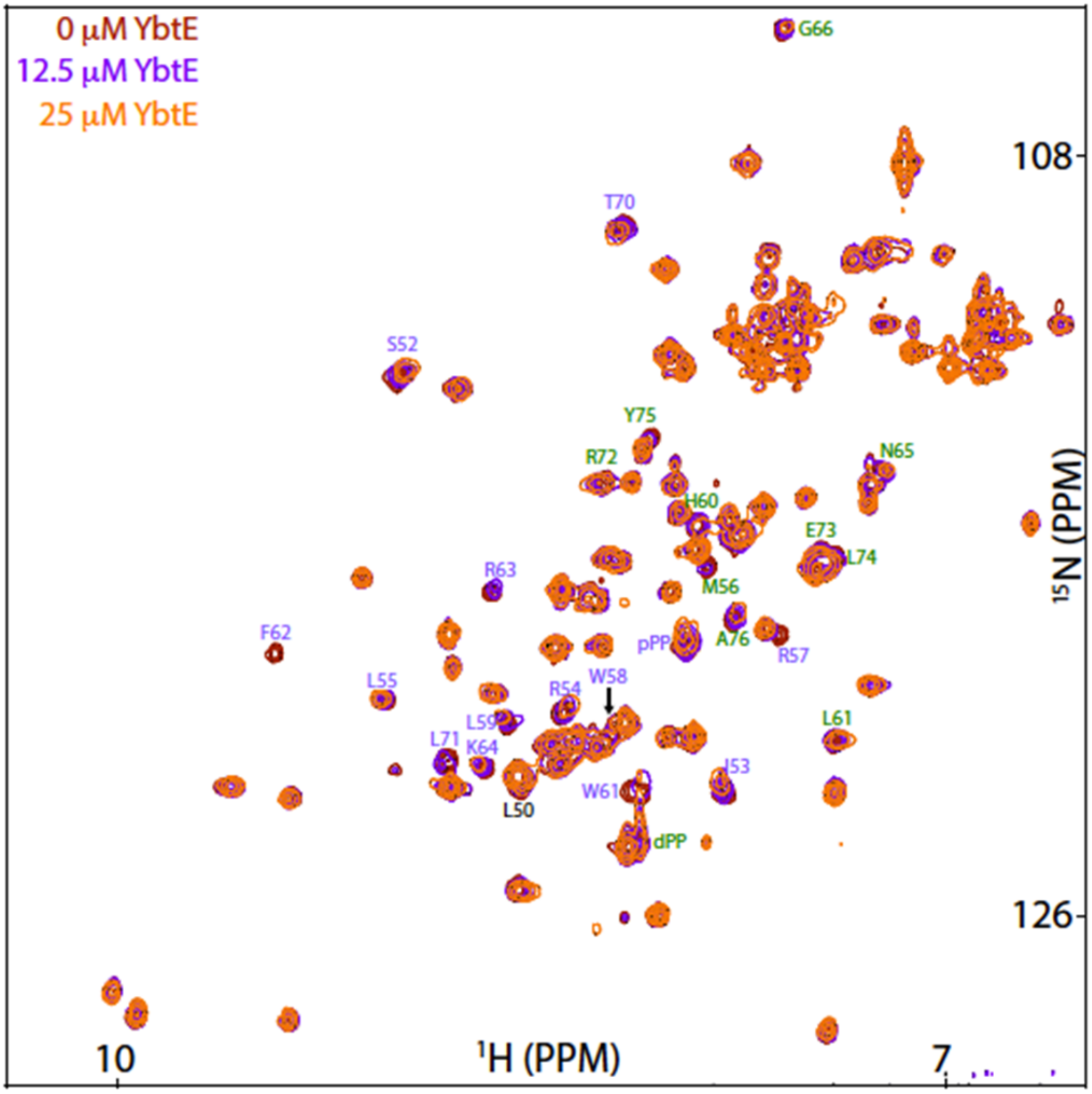

Figure S15. Overlay of HN-HSQCs collected during titration of holo-ArCP with YbtE. Residues that showed a CSP greater than 1 standard deviation (STDEV) above the mean are labeled in black, those that showed a R_{int} greater than 1 STDEV above the mean are labeled in green, and those that showed a CSP and R_{int} that were both greater than 1 STDEV above the mean are labeled in lavender.

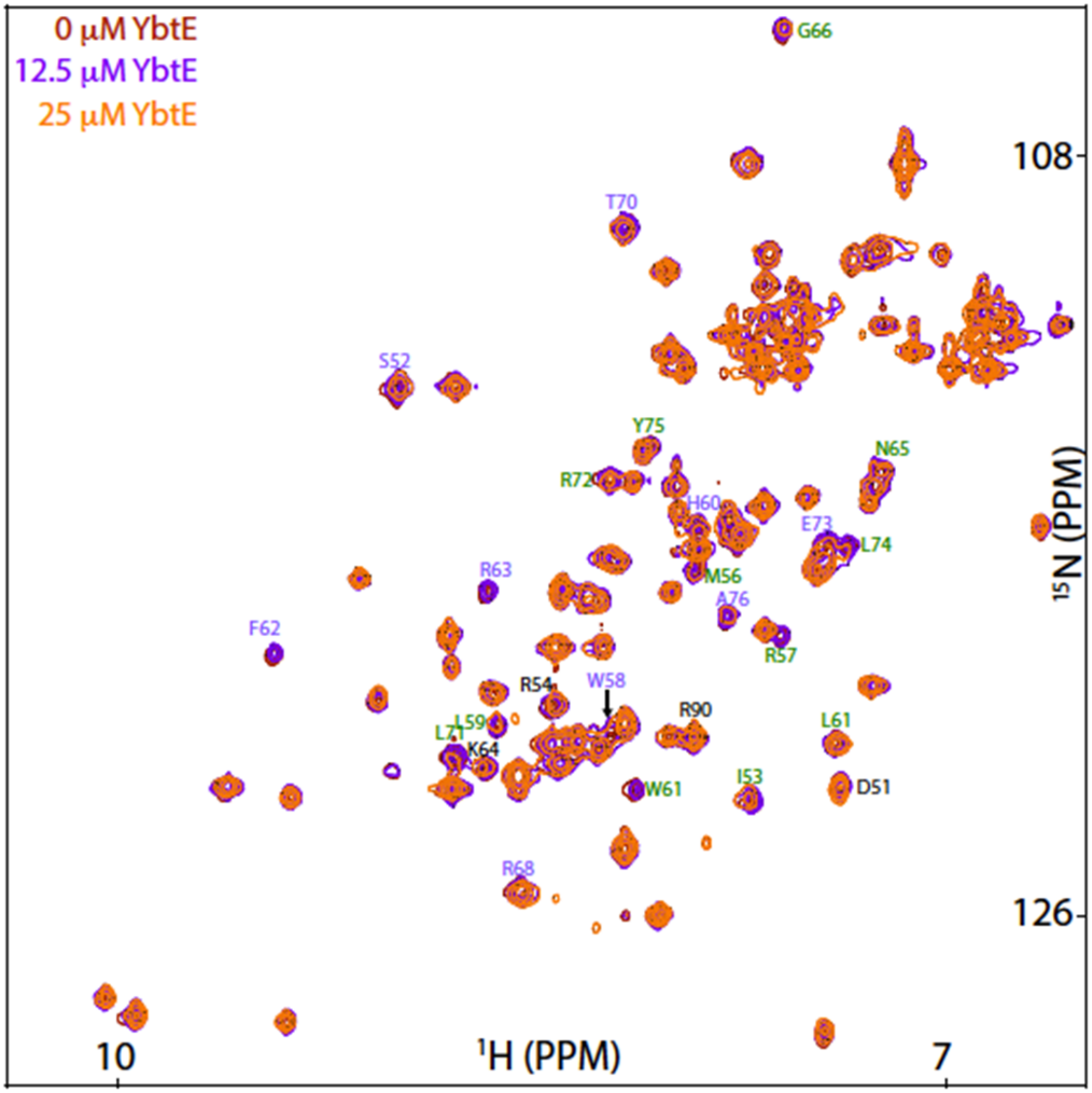

Figure S16. Overlay of HN-HSQCs collected during titration of SalNH-ArCP with YbtE. Residues that showed a CSP greater than 1 standard deviation (STDEV) above the mean are labeled in black, those that showed a R_{int} greater than 1 STDEV above the mean are labeled in green, and those that showed a CSP and R_{int} that were both greater than 1 STDEV above the mean are labeled in lavender.

Synthesis of SalNH-pant:

Sodium 2-hydroxybenzoate was coupled to N-Boc-ethylenediamine with HATU to provide amide **1**. Treatment of **1** with excess trifluoroacetic acid (TFA) provided the amine salt **2**. Without further purification, amine salt **2** was coupled with pantothenic dimethyl ketal **3** (7) to provide phenol **4**. Exposure of phenol **4** to aqueous HCl revealed the diol to produce SalNH-pant.

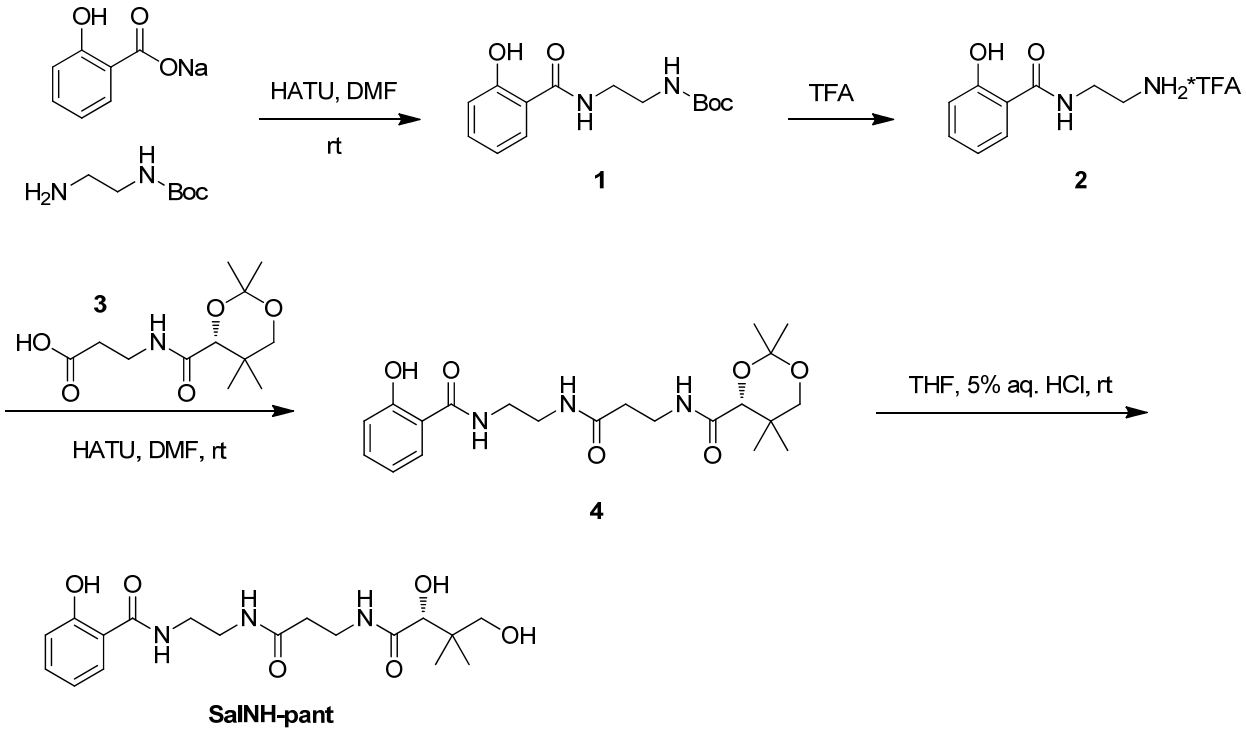

Experimental:

tert-butyl (2-(2-hydroxybenzamido)ethyl)carbamate: To a solution of sodium salicylate (557 mg, 3.47 mmol) and N,N-diisopropylethylamine (1.21 ml, 6.95 mmol) in anhydrous DMF (3.5 ml) was added HATU (1456 mg, 3.83 mmol) in one portion at rt under an argon atmosphere. After stirring for 5 min. at rt, N-Boc-ethylenediamine (0.58 ml, 3.65 mmol) was added in one portion, and the reaction was magnetically stirred at rt an additional 18 h. The reaction was diluted with 15 ml of water and extracted

with EtOAc (3 x 15 ml). The organic layers were combined, washed with brine, dried with anhydrous $MgSO_4$, and concentrated *in vacuo*. Purification by flash chromatography (0 to 10% MeOH/$CHCl_3$) provided 438 mg of **1** as clear colorless oil (45%). Rf = 0.63 (50% EtOAc/Hex). ^{1}H NMR (500 MHz, $CDCl_3$) δ 12.50 (s, 1H), 7.76 (br. s., 1H), 7.47 (d, *J* = 7.70 Hz, 1H), 7.37 (t, *J* = 7.78 Hz, 1H), 6.96 (d, *J* = 8.33 Hz, 1H), 6.79 - 6.89 (m, 1H), 4.99 (br. s., 1H), 3.49 - 3.60 (m, 2H), 3.31 - 3.49 (m, 2H), 1.44 (s, 9H). ^{13}C NMR (126 MHz, $CDCl_3$) δ 170.5, 161.5, 158.1, 134.0, 125.9, 118.6, 118.3, 114.1, 80.4, 42.5, 39.4, 28.3.

N-(2-aminoethyl)-2-hydroxybenzamide TFA salt: To a solution of tert-butyl (2-(2-hydroxybenzamido)ethyl)carbamate (659 mg, 2.35 mmol) in CH_2Cl_2 (2.4 ml) was added TFA (2.4 ml) in one portion at rt. After stirring for 1 h at rt, TLC indicated that all the starting material was consumed. The volatiles were removed *in vacuo* to provide a syrup that was used in the next step without further purification. ^{1}H NMR (500 MHz, CD_3OD) δ 7.78 (dd, *J* = 1.49, 8.10 Hz, 1H), 7.40 (ddd, *J* = 1.73, 7.15, 8.41 Hz, 1H), 6.78 - 6.99 (m, 2H), 3.69 (t, *J* = 5.82 Hz, 2H), 3.17 (t, *J* = 5.74 Hz, 2H).

(R)-N-(3-((2-(2-hydroxybenzamido)ethyl)amino)-3-oxopropyl)-2,2,5,5-tetramethyl-1,3-dioxane-4-carboxamide: To a solution of pantothenic dimethyl ketal **3**(7) (610 mg, 2.35 mmol) and N,N-diisopropylethylamine (1.23 ml, 7.05 mmol) in anhydrous DMF (2.4 ml) was added HATU (894 mg, 3.83 mmol) in one portion at rt under an argon atmosphere. After stirring for 5 min. at rt, a solution of N-(2-aminoethyl)-2-hydroxybenzamide TFA salt (ca. 2.35 mmol) dissolved in a minimal amount of DMF was added in one portion, and the reaction was magnetically stirred at rt an additional 18 h. The reaction was diluted with 15 ml of water and extracted with EtOAc (3 x 15 ml). The organic layers were combined, washed with brine, dried with anhydrous $MgSO_4$, and concentrated *in vacuo*. Purification by flash chromatography (0 to 10% MeOH/$CHCl_3$) provided 394 mg of **4** as clear colorless

glass (40%). Rf = 0.68 (10% MeOH/$CHCl_3$). ^{1}H NMR (500 MHz, $CDCl_3$) δ 12.49 (br. s., 1H), 8.01 (br. s., 1H), 7.54 (d, *J* = 8.02 Hz, 1H), 7.37 (t, *J* = 7.78 Hz, 1H), 6.91 - 7.07 (m, 3H), 6.86 (t, *J* = 7.62 Hz, 1H), 4.07 (s, 1H), 3.67 (d, *J* = 11.63 Hz, 1H), 3.43 - 3.63 (m, 6H), 3.27 (d, *J* = 11.79 Hz, 1H), 2.52 (t, *J* = 6.05 Hz, 2H), 1.41 (d, *J* = 9.12 Hz, 6H), 1.02 (s, 3H), 0.96 (s, 3H).

(R)-N-(2-(3-(2,4-dihydroxy-3,3-dimethylbutanamido)propanamido)ethyl)-2-hydroxybenzamide (SalNH-pant): To a solution of (R)-N-(3-((2-(2-hydroxybenzamido)ethyl)amino)-3-oxopropyl)-2,2,5,5-tetramethyl-1,3-dioxane-4-carboxamide (394 mg, 0.93 mmol) in THF (30 ml) was added 5% aq. HCl (2 ml) at rt. After stirring 18 h at rt, the reaction was diluted with 15 ml of water and extracted with EtOAc (3 x 15 ml). The organic layers were combined, washed with sat. aq. $NaHCO_3$, brine, dried with anhydrous $MgSO_4$, and concentrated *in vacuo*. Purification by flash chromatography (0 to 10% MeOH/$CHCl_3$) provided 85 mg of SalNH-pant as clear colorless oil. ^{1}H NMR (500 MHz, CD_3OD) δ 7.74 (d, J = 7.55 Hz, 1H), 7.24 - 7.51 (m, 1H), 6.89 (dd, J = 4.01, 7.78 Hz, 2H), 3.92 - 4.04 (m, 1H), 3.88 (br. s., 1H), 3.62 - 3.84 (m, 1H), 3.37 - 3.58 (m, 6H), 3.17 (br. s., 1H), 2.58 (t, J = 5.66 Hz, 1H), 2.43 (br. s., 1H), 1.17 (s, 1.5H), 1.01 (s, 1.5H), 0.90 (s, 3H).

References

1. Güntert, P. (2004) Automated NMR structure calculation with CYANA. *Methods Mol. Biol.* **278**, 353–78
2. Bhattacharya, A., Tejero, R., and Montelione, G. T. (2007) Evaluating protein structures determined by structural genomics consortia. *Proteins*. **66**, 778–95
3. Laskowski, R., Rullmann, J. A., MacArthur, M., Kaptein, R., and Thornton, J. (1996) AQUA and PROCHECK-NMR: Programs for checking the quality of protein structures solved by NMR. *J. Biomol. NMR*. 10.1007/BF00228148
4. Koradi, R., Billeter, M., and Wüthrich, K. (1996) MOLMOL: A program for display and analysis of macromolecular structures. *J. Mol. Graph.* **14**, 51–55
5. Walker, O., Varadan, R., and Fushman, D. (2004) Efficient and accurate determination of the overall rotational diffusion tensor of a molecule from (15)N relaxation data using computer program ROTDIF. *J. Magn. Reson.* **168**, 336–45
6. Berlin, K., Longhini, A., Dayie, T. K., and Fushman, D. (2013) Deriving quantitative dynamics information for proteins and RNAs using ROTDIF with a graphical user interface. *J. Biomol. NMR*. **57**, 333–352
7. Gaudelli, N. M., and Townsend, C. A. Stereocontrolled Syntheses of Peptide Thioesters Containing Modified Seryl Residues as Probes of Antibiotic Biosynthesis. 10.1021/jo4007893